Chemical Methodologies 8(2024) 177-199

Chemical Methodologies

Journal homepage: http://chemmethod.com

Original Article

Synthesis of TiO_2/CD and TiO_2/Ag/CD Nanocomposites and Investigation of Their Visible Light Photocatalytic Activities in the Degradation of Methylene Blue

Amirhosein Zamani, Sakineh Asghari*, Mahmood Tajbakhsh*

Department of Organic Chemistry, University of Mazandaran, Babolsar, Iran

ARTICLEINFO

Article history

Submitted: 2023-12-24
Revised: 2024-01-29
Accepted: 2024-02-19
Manuscript ID: CHEMM-2312-1753
Checked for Plagiarism: Yes
Checked Language: Yes

DOI:10.48309/CHEMM.2024.432168.1753

KEYWORDS

β-cyclodextrin
TiO_2 nanocomposites
Photocatalyst
Methylene blue
Visible light

ABSTRACT

The surface of bio-synthesized TiO_2 nanoparticles was modified with a silane agent to generate the chemical link to the preparation of TiO_2/*β*-cyclodextrin and TiO_2/Ag/*β*-cyclodextrin nanocomposites. The structure of synthesized nanocomposites was identified using different techniques, including FTIR, DRS, XRD, ICP, TGA, FESEM, and EDX MAPPING. The photocatalytic activity of the nanocomposites was investigated in the degradation of methylene blue dye in aqueous solution under sunlight irradiation (400-700 nm). The effective factors in the degradation of methylene blue dye including, nanocomposite dosage, initial methylene blue concentration, and irradiation time were studied. The results revealed that under optimum degradation conditions (0.01 g nanocomposite, initial methylene blue concentration of 10 ppm, and 120 min sunlight exposure time), TiO_2/Ag/*β*-cyclodextrin exhibited the highest photocatalytic activity among the tested nanocomposites. The photocatalytic efficiency of nanocomposites showed the order: TiO_2/Ag/*β*-cyclodextrin (99.38%)> TiO_2/*β*-cyclodextrin (84.1%)> TiO_2 nanoparticles (63.76 %). Photocatalytic activity of the synthesized nanocomposites revealed that these materials could be promising candidates for the degradation of various pollutants.

*Corresponding author: Sakineh Asghari and Mahmood Tajbakhsh
E-mail: s.asghari@umz.ac.ir and tajbaksh@umz.ac.ir

GRAPHICAL ABSTRACT

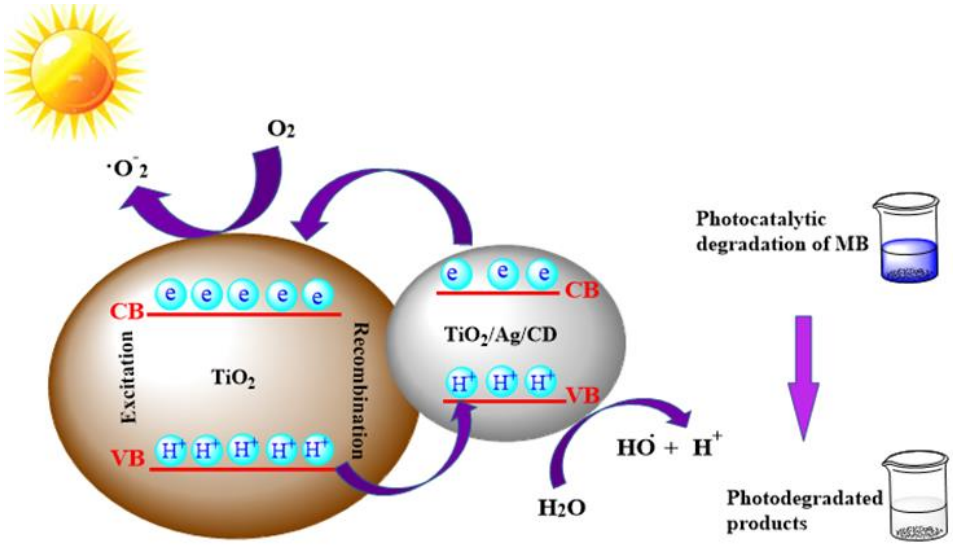

Photocatalytic degradation of methylene blue by TiO_2/Ag/CD

Introduction

A major problem in the world today involves the pollution of water resources by organic pollutants produced by businesses [1,2]. Untreated industrial wastewater contains a large concentration of organic contaminants, which can be harmful to the environment and human health [3,4]. One important class of pollutants is the presence of dyes in wastewater. Methylene blue (MB) is one of the most widely used dyes, and produces large amounts of organic pollutants Methylene blue (MB) is utilized in various sectors, including paper, printing, textile, and food, and as a result, it is an important organic pollutant. In addition, as MB dye is a carcinogenic, harmful, and mutagenic pollutant [5], it is crucial to remove this pollutant from aquatic systems. To date, many chemical, physical, and biological techniques for removing these pollutants from wastewater have been developed [6-9]. Various adsorbents have been studied to remove dyes from water, and the adsorption approach is thought to be one of the most efficient and straightforward methods among other techniques [10]. For instance, the activated carbon is frequently employed and is thought to be a superior adsorbent. However, because of high cost of regeneration, it was occasionally used as a one-time adsorbent [9]. The resistant nature of synthetic dyes renders ineffectual traditional biological treatment procedures, and using adsorption, coagulation, or sedimentation techniques leads to additional contaminants [11].

As a result, a more promising method for the decolorization and degradation of textile dyes has been thoroughly explored. This technology is based on oxidation processes [11]. In this context, scientists are continuously trying to develop cost-effective and efficient semiconductor photocatalysts that limit the use of H_2O_2 under sunlight [5]. In the realm of nanomaterials, the ones that have garnered the most interest are TiO_2 nanoparticles (NPs) because of their chemical properties like high catalytic activity in organic reactions, light absorbing ability, availability, and low price [2, 12]. TiO_2 photocatalyst has been widely used to remove organic pollutants [13].

Due to the outstanding photocatalytic capabilities of TiO_2 NPs, they have found widespread applications in the sewage treatment [14, 15].

The process of decolorization of a dye by TiO_2 catalyst, as a photocatalyst, is explained through electron transformation from the valence band to

the conduction band, which then an electron-hole pair (e^-_{cb} and h^+_{vb}) is generated [16,17].

$$TiO_2 \text{ photocatalyst} + h\nu \longrightarrow e^-_{cb} + h^+_{vb}$$

These species can move to the TiO_2 surface and redox reaction occurs with other species, for example, h^+_{vb} reacts with H_2O on the surface to form active radicals (•OH), whereas the reaction of e^-_{cb} with O_2 generates $O_2^{\bullet-}$ [16,17].

$$H_2O + h^+_{vb} \longrightarrow {}^{\bullet}OH + H^+$$

$$O_2 + e^-_{cb} \longrightarrow O_2^{\bullet-}$$

•OH and $O_2^{\bullet-}$ species reacting with dye to degrade it to small molecules [16,17].

$$H^+ + O_2^{\bullet-} \longrightarrow {}^{\bullet}OOH$$

$${}^{\bullet}OOH + {}^{\bullet}OOH \longrightarrow H_2O_2 + O_2$$

$$H_2O_2 + e^-_{cb} \longrightarrow {}^{\bullet}OH + {}^{-}OH$$

$$dye + {}^{\bullet}OH \longrightarrow {}^{\bullet}dye$$

$${}^{\bullet}dye + ({}^{-}OH + O_2^{\bullet-} + h^+_{vb}) \longrightarrow \text{intermediates} \longrightarrow CO_2 + H_2O$$

Among the three crystalline polymorphic phases of TiO_2, rutile, anatase, and brookite, the anatase phase is the most effective and widely used TiO_2 photocatalyst [18]. However, its high bandgap (3.2 eV) and high rate of charge carrier recombination under visible light make it not an efficient photocatalyst [5, 18-21]. To reduce the energy gap and enhance visible light absorption and photocatalytic performance, TiO_2 has been modified in several ways, including metals or metal oxides [22-24]. non-metals [25,26], organisms [27,28], ionic liquids [29], and miscellaneous compounds like CDs [30,31]. For example, doping of TiO_2 with Fe_3O_4 (8 wt. %) increased the photocatalytic activity of TiO_2 for MB degradation from 75% to 93% under sunlight irradiation [32]. Also, a comparison of the photocatalytic activity of TiO_2 with its composites TiO_2/SiO_2 and TiO_2/SiO_2-CdS exhibited that the activity was increased from 51% (TiO_2) to 74% (TiO_2/SiO_2), and 85% (TiO_2/SiO_2-Cds) in the degradation of MB dye under sunlight irradiation [19]. Nano and microscale silver-based materials with high photosensitivity have been used as TiO_2 doping agents [22, 33-35], which can enhance the photocatalytic activity of TiO_2 under visible light. Cyclodextrins (CDs) are cyclic oligosaccharides made of the hydrophobic interior cavity and the hydrophilic exterior surface. The number of α-D-glucose units in cyclodextrins ranges from six to eight, and they are joined to one another by glycosidic α-1,4 linkages. Several adsorbents that have been functionalized with β-CD have been reported recently to remove harmful pollutants from industrial effluents [36]. Reports showed that the β-CD presence in the photocatalysts structure can increase photodegradation properties because β-CD can interact effectively with organic pollutants. For example, the removal of bisphenol A enhanced in aqueous media in the presence of β-CD [31]. Removal of Cr(VI) and phenol in aqueous solution was increased using rGO/β-CD/TiO_2 nanocomposite [37]. Other examples include graphene oxide and TiO_2 stabilized by β-CD led to improved methylene blue photodegradation [38], and β-CD/Fe_3O_4/TiO_2 also exhibited to be an efficient catalyst in photodecomposition of bisphenol A and dibutyl phthalate [39].

Methylene blue has an amphiphilic nature, as it can interact with hydrophobic and hydrophilic sections of *β*-CD. The positive nitrogen of methylene blue may also form electrostatic interactions with the oxygen atoms on the hydrophilic surface. According to the dimensions of methylene blue molecules and the hydrophobic cavity of β-cyclodextrin, MB may enter a *β*-cyclodextrin cavity and thus be absorbed, or several *β*-cyclodextrin cavities simultaneously enclose an MB molecule and through chemical interaction cause the MB absorption (Figure 1) [40,41].

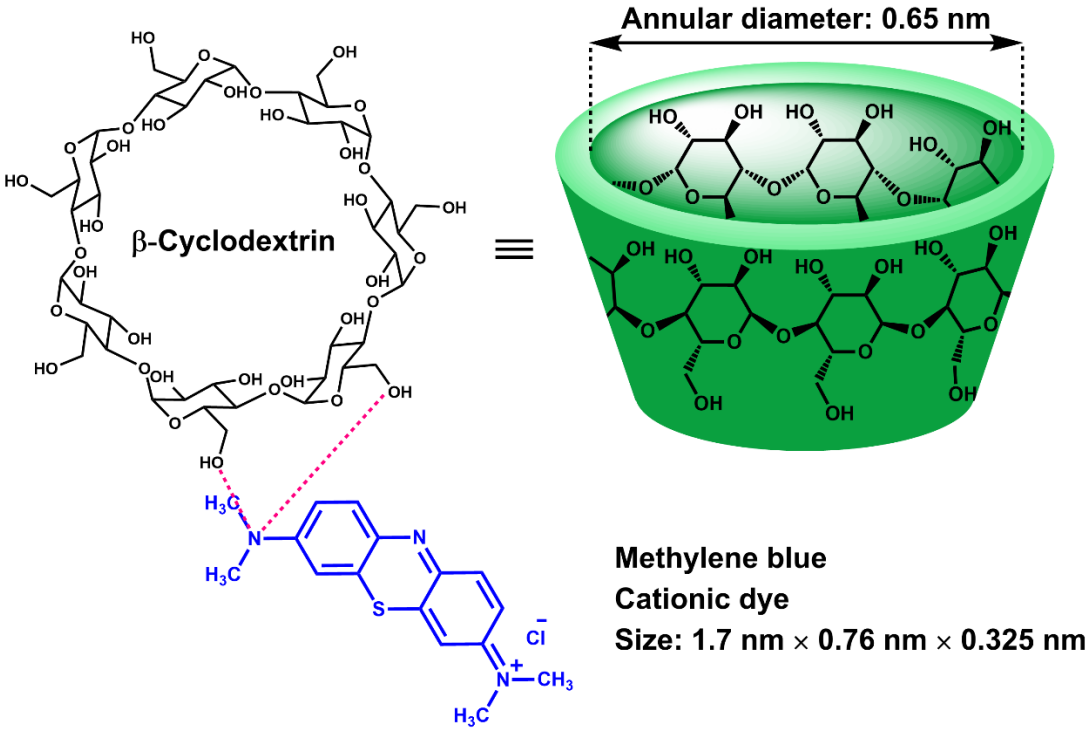

Figure 1: The interaction of methylene blue and beta-cyclodextrin

Herein, we report the synthesis and characterization of TiO_2/*β*-cyclodextrin (TiO_2/CD) and TiO_2/Ag/*β*-cyclodextrin (TiO_2/Ag/CD) nanocomposites and the evaluation of their photocatalytic activity in the degradation of MB in aqueous solutions.

The covalently bounded CD to the modified TiO_2/Ag and/or TiO_2 NPs would enhance the stability and performance of photocatalytic activity of the prepared nanocomposites in the degradation of methylene blue in aqueous solution.

Experimental

Materials and Methods

Titanium chloride ($TiCl_4$), ethanol, deionized water (DW), *β*-cyclodextrin (CD), bromine, dimethyl sulfoxide (DMSO), *N,N'*-dimethylformamide (DMF), triphenylphosphine (PPh_3), silver nitrate ($AgNO_3$), 3-aminopropyltrimethoxysilane (APTMS), diethyl ether, and dichloromethane were obtained from Sigma-Aldrich and Merck Chemical Companies and used unpurified.

The UV-Visible absorption spectra were recorded using a spectrophotometer from Analytik Jena (SPEKOL 2000). A Bruker Tensor 27 Spectrometer was used to record IR spectra using the KBr disc technique. DRS analysis was performed via a Diffuse Reflectance Spectroscopy (DRS, S_4100 SCINCO). A D8 Advance-Bruker X-ray diffractometer was utilized under Cu-Kα radiation (λ = 1.54178 Å) to study the crystal structure of samples. Thermogravimetric analysis (TGA, STA 1500 Rheometric Scientific) was performed at 25 to 600 °C with a heating rate of 10 °C min^{-1} in an air atmosphere. Field

emission scanning electron microscopy (FESEM; MIRA3 Tescan, Switzerland) was used to study examine the surface morphology of synthesized materials. Energy-dispersive X-ray mapping spectroscopy (EDX-MAP, MIRA2 Tescan, Switzerland) was utilized to record elemental detection with sufficient sensitivity to determine the corresponding atomic numbers. Inductive Coupled Plasma- Mass Spectrometry (ICP-MS Agilent 7500) ELAN 6100 DRC-e was used to measure determine the Ti and Ag contents of the TiO_2/CD and TiO_2/Ag/CD nanocomposites.

Preparation of Aloe Vera Extract

The healthy leaves of the Aloe Vera plant were harvested and thoroughly washed to remove dust and impurities. Then, the leaves were washed again with distilled water and left to dry at room temperature. Aloe Vera leaves were chopped, the inside gel was collected (100 g), and heated in distilled water (250 mL) for 2 h at 80 °C. The aqueous mixture was filtered and the filtrate was kept at 10 °C [42].

TiO_2 Anatase NPs Biosynthesis

An aqueous Aleo Vera extract (20 mL) was added slowly to an aqueous solution of $TiCl_4$ (100 mL, 1 M) with vigorous stirring (pH~7). The reaction mixture was stirred for 4 h at room temperature. The obtained TiO_2 NPs were collected by centrifugation (10,000 rpm) and washed several times with ethanol and water. Then dried at 100 °C for 7 h. The solid powder was calcined at 500 °C for 3 h, and a soft white powder was obtained [42,43].

Preparation of C.pentagyna Extract

Fresh fruit was thoroughly rinsed with sterile double-distilled water to eliminate any medium components from the biomass. Then, 50 g of *C.pentagyna* fruit was extracted by maceration using 300 milliliters of methanol as the extraction solvent at room temperature. The methanolic solution was subsequently filtered and concentrated using a rotary evaporator until a rudimentary solid extract was obtained. The extract was filtered and stored at 4 °C. The final extract was utilized as a capping and reducing agent in the synthesis of silver nanoparticles [44].

Biosynthesis of TiO_2/Ag Nanoparticles (TiO_2/AgNPs)

A mixture of TiO_2 nanoparticles (0.5 g, 6.26 mmol) and silver nitrate (0.31 mmol, 0.053 g) was stirred in distilled water (25 mL) for 35 min, then *C. pentagyna* aqueous fruit extract (12.5 mL, pH=12) was added slowly to the mixture and refluxed for 5 h. The white nanoparticles turned black, indicating the reduction of Ag^+ to Ag^0 and the formation of TiO_2/Ag nanoparticles, which were then centrifuged (10,000 rpm) for 10 min, washed with distilled water, and dried in an oven for 24 h [44,45].

TiO_2/Ag Nanoparticles Modification

TiO_2/Ag (0.5 g) was suspended in 50 mL of deionized water (DI) and ultrasonicated for 10 min. The dispersion was then treated with a silane coupling agent (APTMS, 2 mL), and the mixture was refluxed for 24 h. After that, the dispersed particles were centrifuged (10 min at 10,000 rpm) and washed with ethanol and water to remove unreacted silane. Before centrifuging the solid particles were ultrasonicated for 10 min to ensure a well-dispersed suspension was restored. Following the completion of the operation, the collected particles were dried in an oven at 100 °C for 24 h [46].

TiO_2 Nanoparticles Modification

TiO_2 nanoparticles (0.5 g) were suspended in DI water (50 mL) and ultrasonicated for 10 min. APTMS (2 mL) was added and refluxed for 24 h. Then the reaction mixture was centrifuged (10 min at 10,000 rpm) and washed with ethanol and water to remove unreacted silane. The collected solid was dried in an oven at 100 °C for 24 h [46].

Synthesis of Heptakis(6-bromo-6-deoxy)-β-cyclodextrin (CDBr)

A solution of bromine (4 mL, 77.6 mmol) in DMF (15 mL) was slowly added to a cold solution (ice bath) of PPh_3 (20.35 g, 77.6 mmol) in DMF (60 mL) and stirred. After 30 min, 4.2 g (3.7 mmol) of dry CD was added, and the reaction mixture was agitated at 80 °C for 15 h. Under a high vacuum, the mixture was concentrated to half its original volume, and the pH was adjusted to 9-10 using fresh CH_3ONa/CH_3OH (3 M, 60 mL) and immediately refrigerated for 30 min. Then reaction mixture was warmed to ambient temperature, stirred for 30 min, and poured into cold water. The reaction mixture was filtered and the precipitate was washed consecutively with water, ether, and dichloromethane and dried overnight in a vacuum to give a quantitative yield of the desired product (5.7 g).

Synthesis of Titanium-Silver Modified Cyclodextrin Nanocomposite (TiO_2/Ag/CD)

CDBr (0.59 mmol, 1 g) was dissolved in DMSO (30 mL) at 95 °C after stirring for 1 h. APTMS-modified TiO_2/Ag nanoparticles (4.14 mmol ~ 1.3 g) were added to the reaction solution, which was then stirred for 24 h at 80 °C. After reaching room temperature, the resulting mixture was transferred to 200 mL of water with stirring. The precipitate was filtered off, rinsed with water, and then dried in a vacuum oven at 90 °C for 24 h to yield TiO_2/Ag/CD nanocomposite with a mass yield of 97% [47].

Synthesis of Titanium-Modified Cyclodextrin Nanocomposite (TiO_2/CD)

CDBr (0.59 mmol, 1 g) was dissolved in DMSO (30 mL) at 95 °C after stirring for 1 h, and then APTMS-modified TiO_2 (1.3 g) was added to the solution and stirred at 80 °C for 24 hours. Afterwards, the reaction mixture was cooled to room temperature and transferred to 200 mL of water with stirring. The precipitate was filtered off, rinsed with water, and then dried in a vacuum oven at 90 °C for 24 h to yield 93% TiO_2/CD nanocomposite [47].

Hotocatalytic Process

An aqueous MB solution was chosen as the contaminant solution model to evaluate the photocatalytic activity of the prepared TiO_2/Ag/CD under sunlight irradiation. 10 mg of photocatalyst was dispersed in a 10 ppm MB solution (100 mL) using an ultrasonic bath, and then stirred for 60 min in the dark to establish the equilibrium of adsorption and desorption between the photocatalyst and MB dye. Next, the solution was exposed to the sunlight and 5 mL of the solution was sampled every 15 minutes using a pipette. The suspension solution was centrifuged, the nano photocatalyst was separated, and the MB concentration was measured using a UV-Vis spectrophotometer at 665 nm [48].

Results and Discussion

In this work, anatase TiO_2 nanoparticles were synthesized by addition of aqueous Aloe vera leaf extract to a solution of $TiCl_4$ in water followed by residue calcination at 500 °C (Scheme 1).

TiO_2/Ag NPs were prepared by mixing TiO_2 NPs with $AgNO_3$ in the presence of *C. pentagyna* aqueous fruit extract at pH=12 as shown in Scheme 2.

Modification of TiO_2/Ag NPs with APTMS in deionized water afforded compound (**1**), which then reacted with CDBr (**2**) (prepared by bromination of CD with Br_2 and pph_3 in DMF) in DMSO to give the nanocomposite TiO_2/Ag/CD in 97% mass yield (Scheme 3).

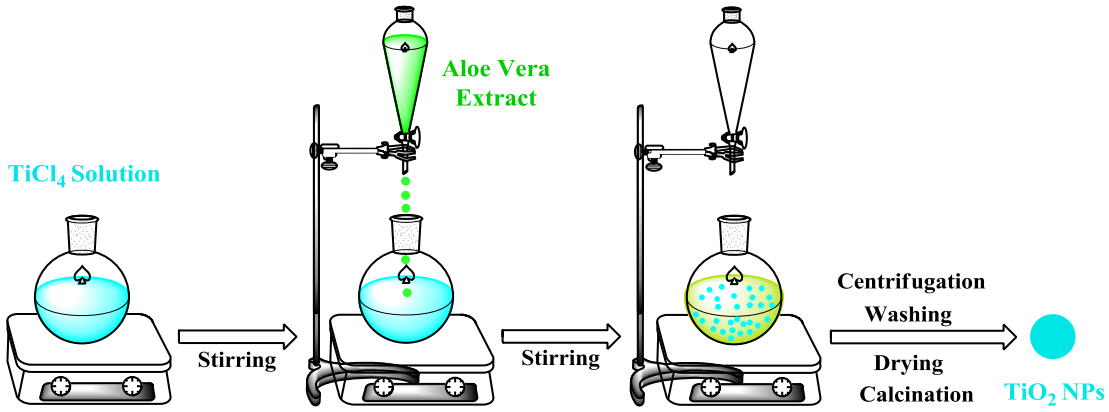

Scheme 1: Biosynthesis of anatase TiO_2 nanoparticles

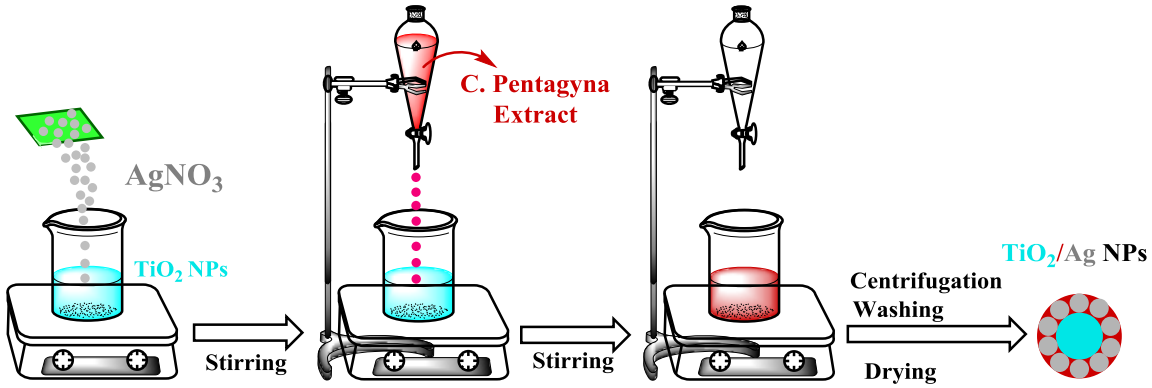

Scheme 2: Biosynthesis of TiO_2/Ag nanoparticles

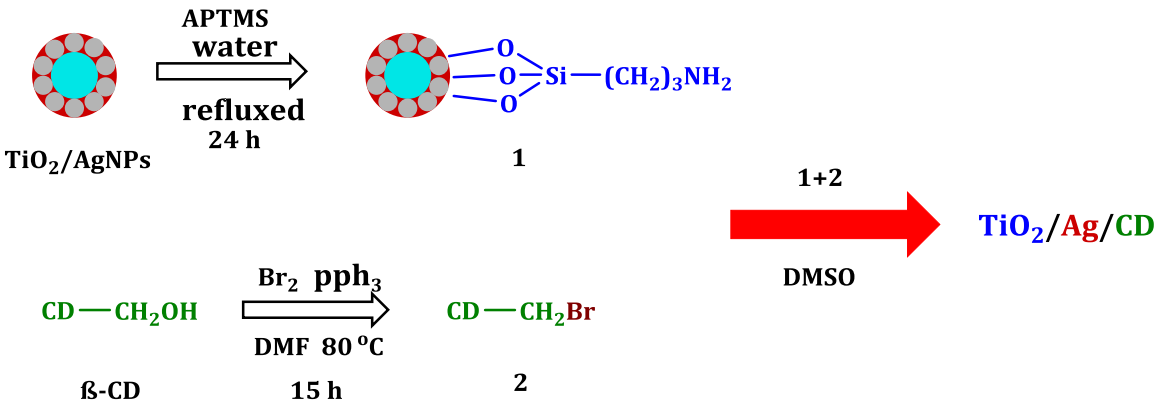

Scheme 3: Synthesis steps of TiO_2/Ag/CD nanocomposite

Similarly, TiO_2 NPs were modified with APTMS followed by reacting with CDBr (**2**) to obtain TiO_2/CD nanocomposite. FT-IR, UV, TGA, DRS FESEM, ICP, EDX, MAP, and XRD were used to identify the structure and morphology of nanocomposites.

FTIR Analysis

Figure 2 depicts the FTIR spectra of β-CD, β-CD-Br, TiO_2, TiO_2/CD, and TiO_2/Ag/CD.

β-CD: 3417.4 cm^{-1} (O-H stretching), 1641.2 cm^{-1} (O-H bending), 2927.5 (C-H stretching), 1419.4

and 1369.2 cm^{-1} (C-H bending), 1157.1, 1081.9, and 1029.8 cm^{-1} (C-O and C-O-C stretching), and 946.9 cm^{-1} (R-1,4 bond skeleton vibration) [49].

CD-Br: Characteristic peaks of β-CD, 1263.2 cm^{-1} (C-Br stretching), and 586.2 cm^{-1} (C-Br bending) [47].

TiO_2: 3600–3300 cm^{-1} (O-H stretching), 1633.4 cm^{-1} (O-H bending), and 500-800 cm^{-1} (Ti-O-Ti stretching) (50, 47].

APTMS modified TiO_2 NPs: 3448 cm^{-1} (NH_2 stretching), 2927.8 cm^{-1} (C-H stretching), 1627.8 cm^{-1} (O-H bending), 1544.9 and 1459 cm^{-1} (Si-O-C characteristic peaks), 1130.2 cm^{-1} (Si-O-Si stretching), and 999 cm^{-1} (Ti-O-Si stretching) [47]. The FTIR spectra of TiO_2/Ag/CD and TiO_2/CD contain all the of the anticipated absorption peaks related to cyclodextrin and TiO_2 moieties.

TiO_2/Ag/CD and TiO_2/CD: The spectra exhibited all the related peaks of TiO_2 and *β*-CD.

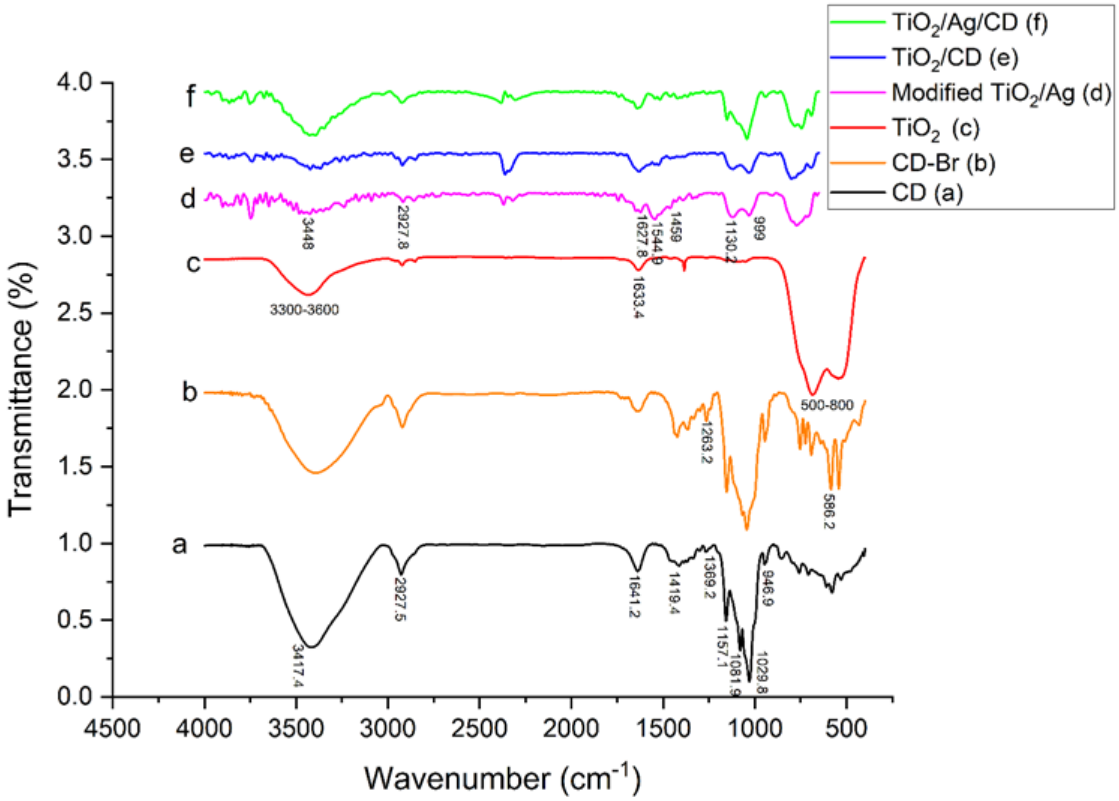

Figure 2: The FTIR spectrum of the synthesized products

EDX Mapping and DRS Analysis

The components of the composites were identified using energy-dispersive X-ray analysis (EDX) and determined the approximate amount of carbon, nitrogen, silicon, silver, titanium, and oxygen elements (Figure 3). The results showed that the quantity of carbon and oxygen in the silver-containing composite is greater. This shows that the TiO_2/Ag/CD composite has more cyclodextrin. According to the DRS analysis results, the energy gap of TiO_2 was 3.2ev, which decreased to 3.1ev and 2.5ev in TiO_2/CD and TiO_2/Ag/CD, respectively. The lowering of the energy gap in the silver-containing composite is expected to make it softer and more reactive with cyclodextrin [5, 47, 51].

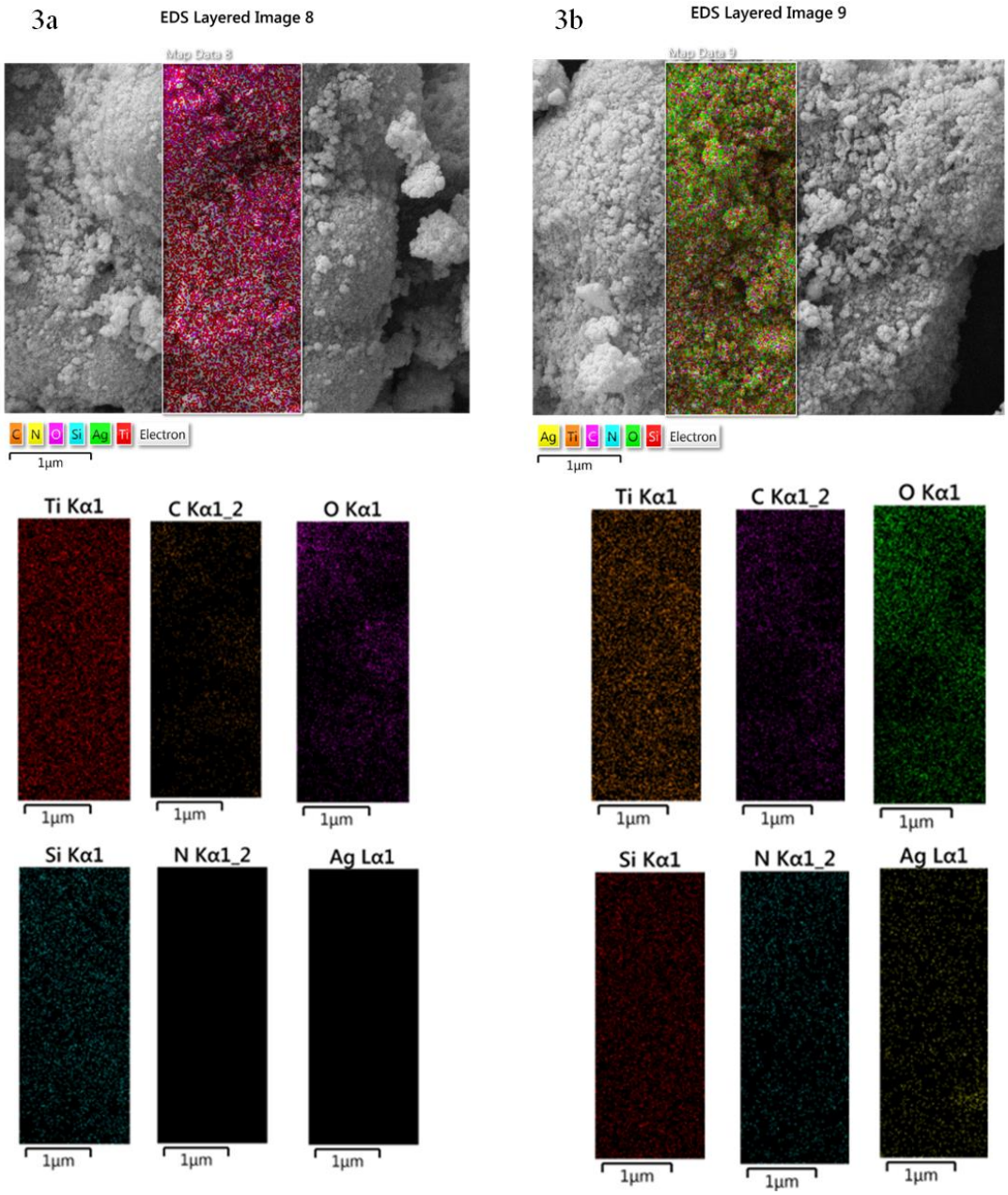

Figure 3: EDX and MAPPING images 3a related to TiO_2/CD and 3b related to TiO_2/Ag/CD

TGA and ICP Analysis

TGA was used to assess the thermal stability of the nanocomposites. The TiO_2 nanoparticles TGA curve reveals that the nanoparticles are stable up to 600 ºC (Figure 4a). Thermal degradation of CD begins at > 250 ˚C, and pyrolysis occurs at > 300 ºC (Figure 4b). The weight of synthetic composites decreases with rising temperature in proportion to the amount of organic chemicals present. In the TGA curve of TiO_2/CD two weight losses are observed (Figure 4c). The first weight loss occurs at <150 °C which is related to the removal of surface water. The second weight loss is seen at 200-600 °C, which could be because of pyrolysis of organic moieties (CD and silane agent). The TGA curve of TiO_2/Ag/CD exhibits two weight reductions at <120 °C and 150-600 °C, which is attributed to the loss of surface water and organic moieties (CD and silane agent), respectively (Figure 4d). The lower char yield of TiO_2/Ag/CD compared with TiO_2/CD is due to the higher amount of CD in its structure.

The amounts of Ag and Ti in the structure of TiO_2/Ag/CD nanocomposite were measured using ICP analysis Ag=6% and Ti= 35%. The Ti percentage in the TiO_2/CD was also determined by ICP analysis to be 66% [52].

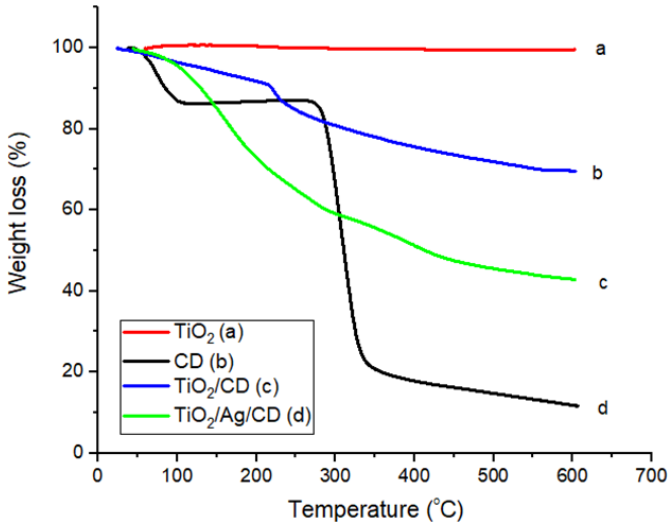

Figure 4: TGA variation diagram of synthesized samples

XRD Analysis

Figure 5 presents the XRD patterns of TiO_2 NPs (anatase), TiO_2/CD, and TiO_2/Ag/CD. All patterns exhibited strong peaks at 2θ = 25.2°, 37.8°, 48°, 54.04°, and 55.1° related to 101, 004, 200, 105, and 211 lattice planes, respectively, confirmed the TiO_2 anatase phase [53,54] . In addition, the peaks of Ag were not clear, which could be because of low silver content in the composite or the (111) reflection of Ag might be overlapped with the (101) reflection of anatase TiO_2 [53]. However, the intensity of diffraction peaks of anatase TiO_2 nanoparticles in TiO_2/Ag/CD nanocomposite decreases with the addition of silver, which could be due to the presence of silver nanoparticles. XRD analysis of β-CD, anatase TiO_2 nanoparticles, and TiO_2/CD and TiO_2/Ag/CD was enhanced for better distinction in patterns by enlarging Figures 6b-e [54-58]. In Figure 6b, two green peaks are observed for the TiO_2/Ag/CD in the 2θ ranges from 21 to 24 degrees, which is related to the presence of a significant amount of cyclodextrin in this nanocomposite.

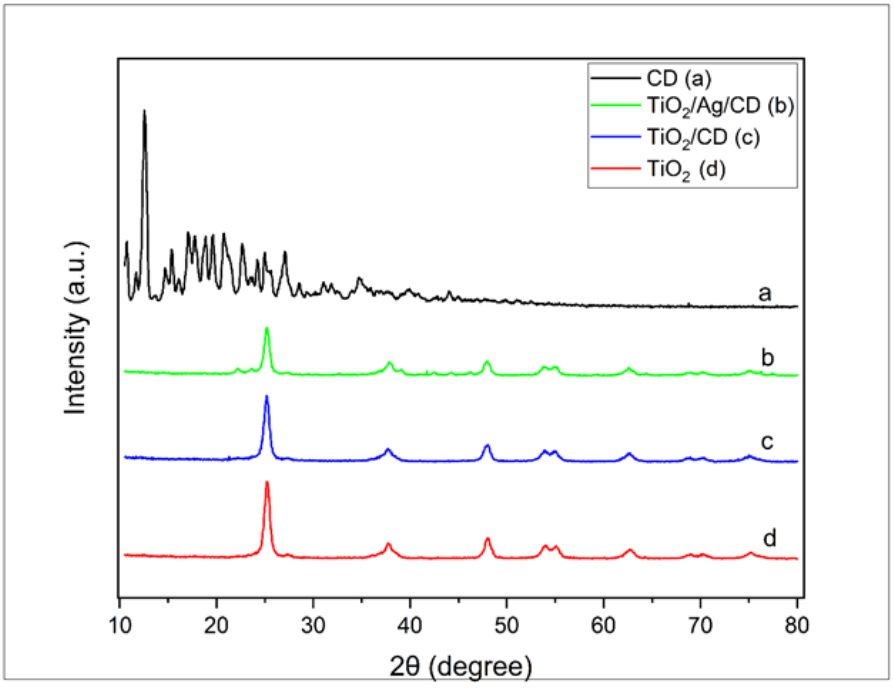

Figure 5: XRD patterns of TiO_2, CD, TiO_2/CD, and TiO_2/Ag/CD

In Figure 6d, we can see small green peaks for the TiO_2/Ag/CD in the 2θ ranges from 39 to 47 degrees, which corresponds to the presence of a significant amount of cyclodextrin in this nanocomposite. Although the presence of CD in TiO_2/CD has been confirmed in other analyses, the characteristic peaks of the CD are significantly less or not seen, which is due to the lower amount of cyclodextrin in the TiO_2/CD relative to TiO_2/Ag/CD.

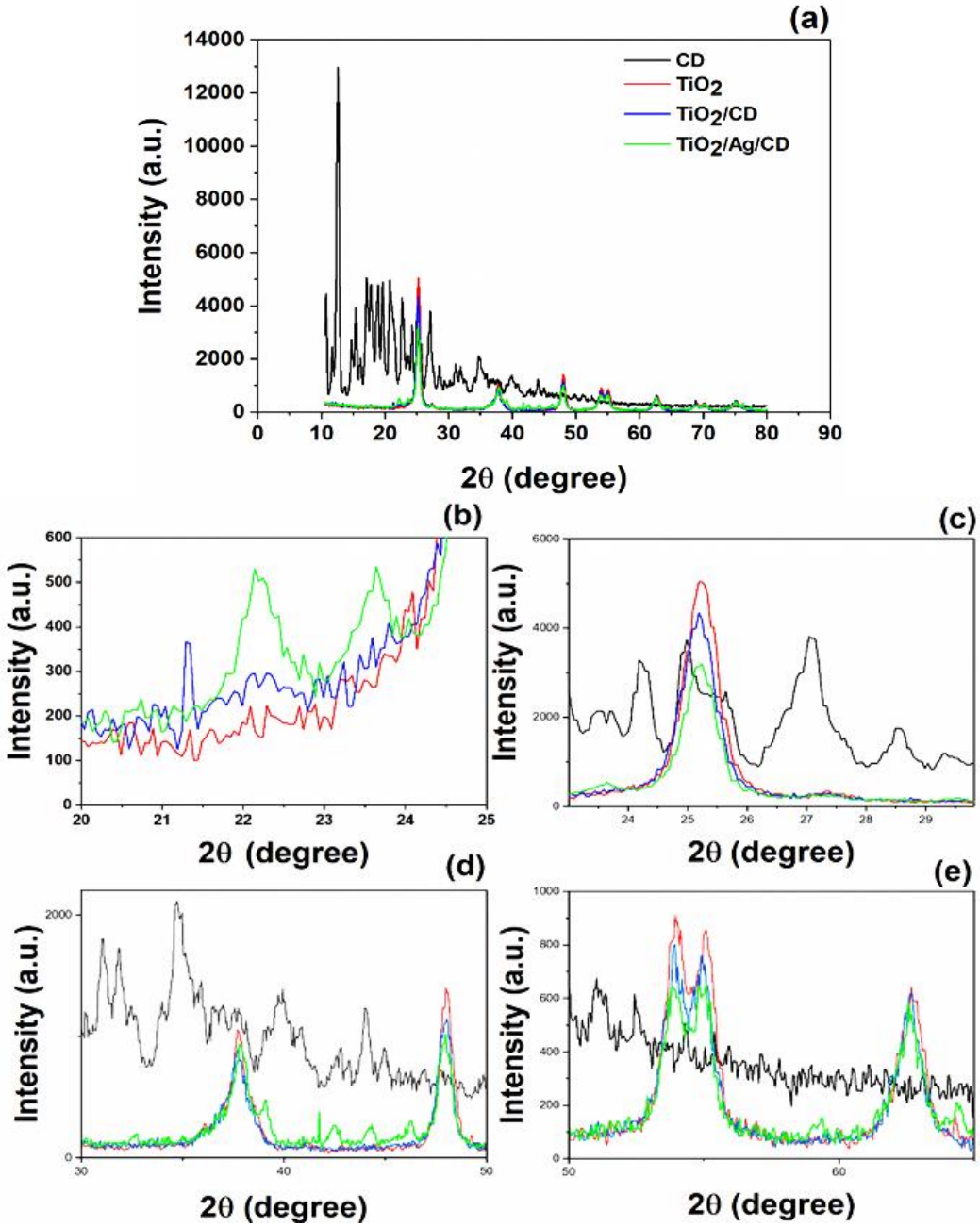

Figure 6: Magnified images of XRD analysis related to *β*-CD, anatase TiO_2 nanoparticles, and TiO_2/CD and TiO_2/Ag/CD

FESEM Analysis

The electron microscope is one of the most powerful and efficient techniques for examining the surface morphology of nanoparticles and nanocomposites. Therefore, FESEM images with a magnification of 500 nm for TiO_2, CD, TiO_2/CD, and TiO_2/Ag/CD are shown in Figure 7. FESEM images of CD show that CD has a smooth, dense, and amorphous surface morphology. On the

other hand, it can be seen from the images related to TiO_2 nanoparticles that TiO_2 has a spherical and relatively rough surface morphology. After modifying the surface of TiO_2 nanoparticles, changes were made in the roughness and compactness of the particles, so that it is clear that a more compact and relatively smoother structure has been created in the TiO_2/CD nanocomposite than the TiO_2 nanoparticles. Through the Ag introduction onto the TiO_2 surface and the subsequent formation of the TiO_2/Ag/CD nanocomposite, it becomes evident that the surface morphology exhibits a higher degree of homogeneity, smoothness, and density compared to that of the TiO_2/CD nanocomposite. In essence, it appears that a greater quantity of the CD exists inside the TiO_2/Ag/CD system, which is consistent with the TGA results. In contrast, the more uniform and stronger binding of CD to the TiO_2 core can increase the efficiency of the nanocomposite in terms of photocatalytic performance.

Based on the findings obtained from the FESEM observations, it can be deduced that the incorporation of silver Ag for surface modification of titanium dioxide TiO_2 exerts a notable impact, specifically a synergistic effect, on the formation and efficacy of robust interactions between the core and CD. Consequently, this leads to the development of a nanocomposite possessing a more homogeneous and enduring structure throughout the synthesis procedure [47].

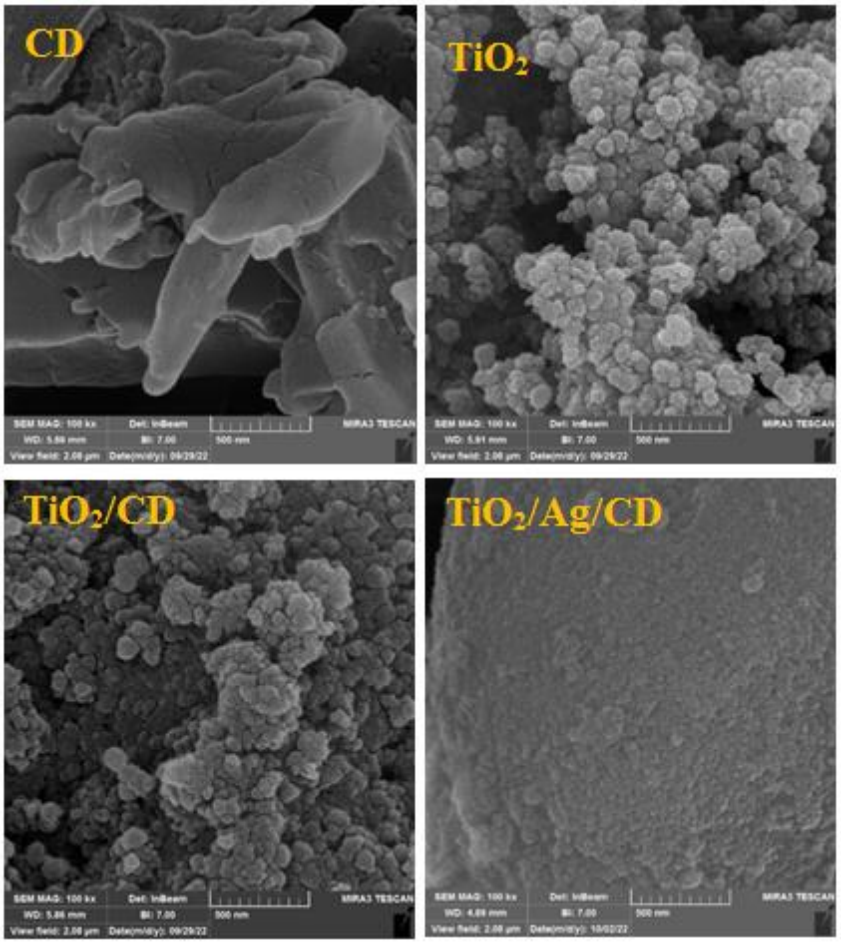

Figure 7: FESEM images with a magnification of 500 nm for TiO_2, CD, TiO_2/CD, and TiO_2/Ag/CD

Using the Figure 8 and origin programs, the dimensions of the produced nanoparticles and nanocomposites were measured and their histograms were drawn (Figure 8).

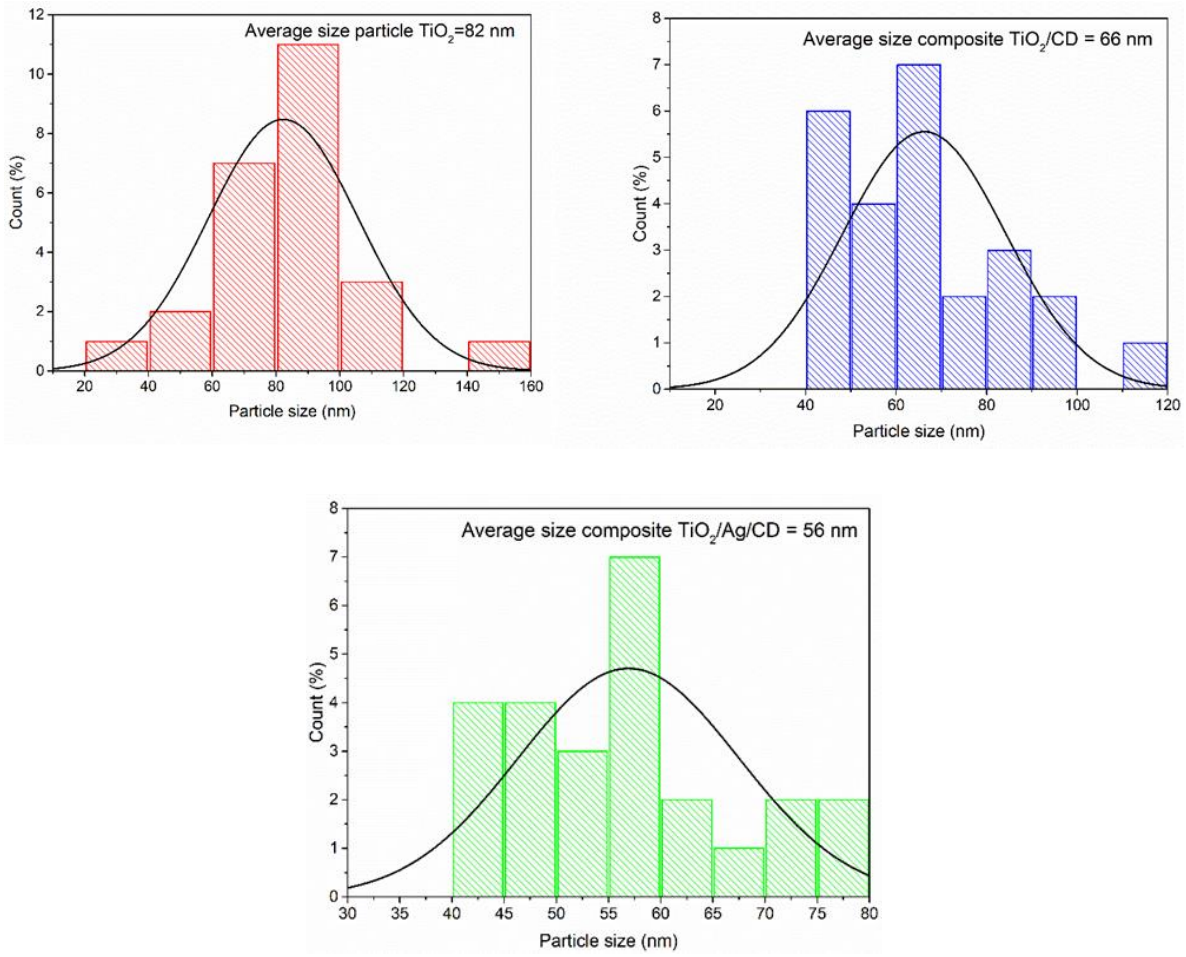

Figure 8: Calculation of the size of nanoparticles using a histogram chart

Photocatalytic Studies

According to the obtained data related to the structural analysis of the produced nanocomposites, it was predicted that TiO_2/Ag/CD would show a better photocatalytic effect than TiO_2 and TiO_2/CD because it contains more CD in its structure and also the presence of silver, which reduced the energy gap leading to facilitate the visible light adsorption. Preliminary experiments were conducted to verify this prediction. The results of the experiments exhibited the order of photocatalytic activity to be: TiO_2/Ag/CD > TiO_2/CD > TiO_2. However, the photocatalytic investigation is explained for the TiO_2/Ag/CD nanocomposite to determine the optimal conditions in the following sections. All the experiments were repeated in triplicate and the reported values are the mean values.

Optimization of Dye Concentration

The optimum initial concentration of dye solution on the removal percentage was investigated at a dosage of 0.01g TiO_2/Ag/CD and 100 mL of the dye solution for a photocatalysis period of 105 min. For this purpose, the dye solutions were initially mixed with 0.01 g of photocatalyst for 1 h in the dark until the adsorption and desorption equilibrium of the photocatalyst and MB dye was established. Then the solutions were exposed to sunlight for 105 min. Figure 9 and Table 1 indicates that the degradation percentage increases with decreasing the initial dye concentration. Percentage degradation values of 99.35, 98.18, 91.29, and 82.93% were obtained for 5, 10, 15, and 20 ppm dye solutions, respectively.

As can be seen in Figure 9, the dye concentration of 5 ppm was slightly better than the 10 ppm solution, thus 10 ppm initial concentration was

chosen as the optimum value for further experiments.

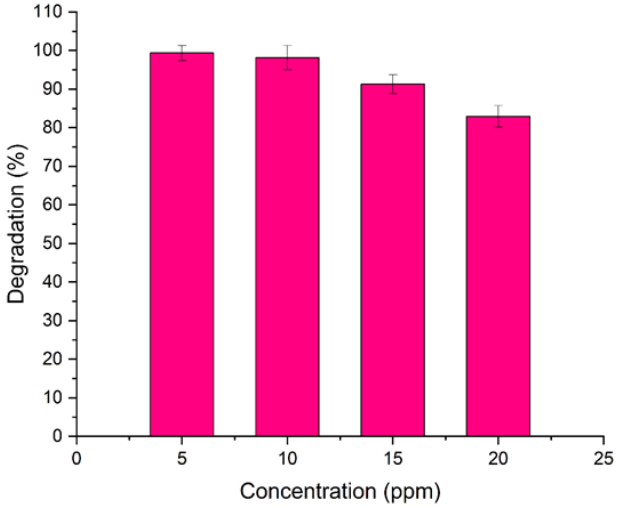

Figure 9: Effect of initial dye concentration on its degradation, C_o=5, 10, 15, 20 ppm, 0.01g TiO_2/Ag/CD, 100 mL, 105 min

Table 1: Optimization of dye concentration

Catalyst	Dosage	Color concentration (ppm)	Time (min)	Degradation (%)
TiO_2/Ag/CD	0.01 g/ 100 mL	5	105	99.35
TiO_2/Ag/CD	0.01 g/ 100 mL	10	105	98.18
TiO_2/Ag/CD	0.01 g/ 100 mL	15	105	91.29
TiO_2/Ag/CD	0.01 g/ 100 mL	20	105	82.93

Optimum contact time

The MB degradation at different contact times is demonstrated in Figure 10 and Table 2. The degradation by 0.01 g of TiO_2/Ag/CD in 100 mL of 10 ppm dye solution increases continuously with time. This increase continues up to 120 min (99.38% degradation), and then reaches equilibrium. The rapid degradation of MB in the early stages of the process can be attributed to the numerous empty holes of CD and the presence of TiO_2 and silver, which facilitate visible light harvesting.

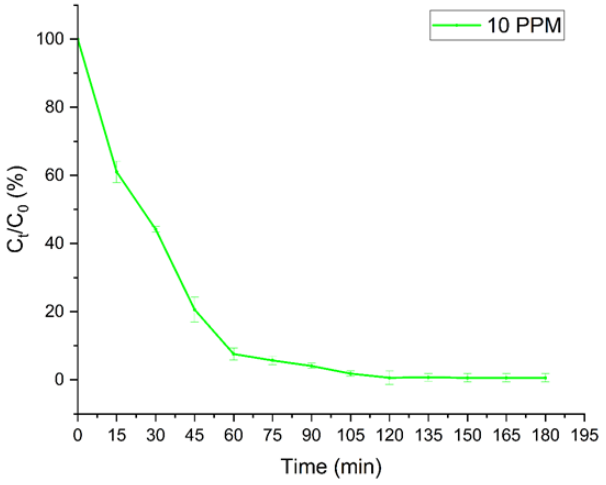

Figure 10: Effects of contact time on the MB degradation, at 0.01g TiO_2/Ag/CD, 100 Ml

Table 2: Optimum contact time

Catalyst	Dosage	Color concentration (ppm)	Time (min)	Degradation (%)
TiO_2/Ag/CD	0.01 g/ 100 mL	10	15	38.96
TiO_2/Ag/CD	0.01 g/ 100 mL	10	30	55.83
TiO_2/Ag/CD	0.01 g/ 100 mL	10	45	79.42
TiO_2/Ag/CD	0.01 g/ 100 mL	10	60	92.43
TiO_2/Ag/CD	0.01 g/ 100 mL	10	75	94.32
TiO_2/Ag/CD	0.01 g/ 100 mL	10	90	95.93
TiO_2/Ag/CD	0.01 g/ 100 mL	10	105	98.18
TiO_2/Ag/CD	0.01 g/ 100 mL	10	120	99.38
TiO_2/Ag/CD	0.01 g/ 100 mL	10	135	99.28
TiO_2/Ag/CD	0.01 g/ 100 mL	10	150	99.44
TiO_2/Ag/CD	0.01 g/ 100 mL	10	165	99.37
TiO_2/Ag/CD	0.01 g/ 100 mL	10	180	99.36

Effect of TiO_2/Ag/CD dosage

The effect of TiO_2/Ag/CD dosage on the MB removal was studied and the results are shown in Figure 11 and Table 3 for initial dye concentrations (0.002, 0.005, 0.01, 0.02, 0.03, and 0.04) g. The degradation percentage was highest at 0.01 mg TiO_2/Ag/CD. It can be seen in this Figure that by increasing the catalyst dosage from 0.002 to 0.005 and 0.01 g the MB degradation percentage increases from 67.40% to 85.6% and then to 99.38% for 0.01 g catalyst. Further increasing the catalyst did not enhance the rate of degradation and even decreased slightly. Therefore, by increasing the amount of catalyst to 0.02, 0.03, and 0.04 g, the degradation percentage was 99.29, 98.76, and 97.42, respectively.

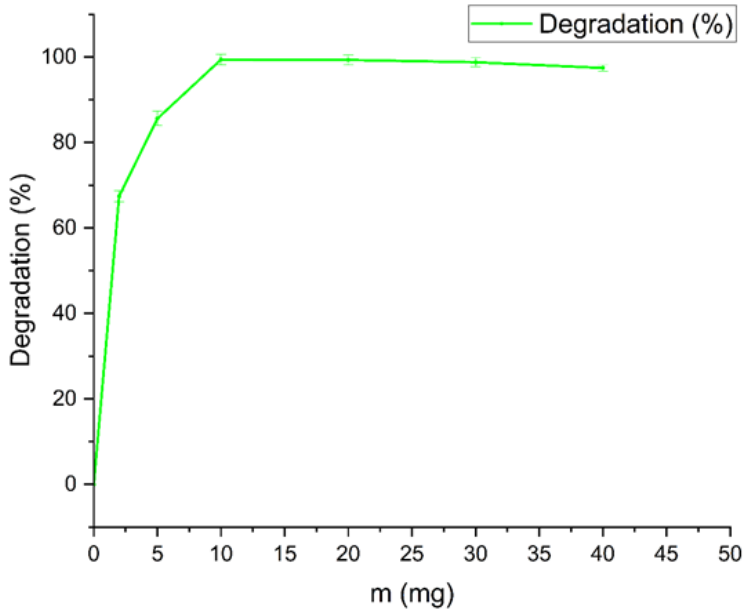

Figure 11: Effects of catalyst dosage on the MB degradation, at different amounts of TiO_2/Ag/CD, 100 mL, 10 ppm dye concentration, 120 min

Table 3: Dose effect of TiO_2/Ag/CD photocatalyst

Catalyst	Dosage	Color concentration (ppm)	Time (min)	Degradation (%)
TiO_2/Ag/CD	0.002 g/ 100 mL	10	120	67.40
TiO_2/Ag/CD	0.005 g/ 100 mL	10	120	85.6
TiO_2/Ag/CD	0.01 g/ 100 mL	10	120	99.38
TiO_2/Ag/CD	0.02 g/ 100 mL	10	120	99.29
TiO_2/Ag/CD	0.03 g/ 100 mL	10	120	98.76
TiO_2/Ag/CD	0.04 g/ 100 mL	10	120	97.42

This might be due to the presence of an excess catalyst, which causes opacity of the mixture, it leads to preventing the passage and penetration of radiated light [16, 59]. As shown in Figure 11, TiO_2/Ag/CD exhibits the highest degradation efficiency at a dose of 0.01 g. Therefore, this value was selected as the optimal dose.

Investigating the Effect of Photocatalyst

Under optimal conditions, the photocatalytic activity of the synthesized TiO_2 nanoparticles, TiO_2/CD, and TiO_2/Ag/CD nanocomposite was evaluated. To ascertain their absorption, three 100 mL solutions of 10 ppm MB were simultaneously mixed with 0.01 g of photocatalyst for 1 h in the dark. After being exposed to sunlight for 120 min, the solutions were sampled each 15 min. Examining the outcomes revealed that, for all three photocatalysts, the quantity of MB degradation increases as contact time increases. During 120 min, Figure 12 and Table 4 demonstrates that TiO_2/Ag/CD, TiO_2/CD, and TiO_2 degraded 99.38%, 84.1%, and 63.76 % of MB, respectively. The greater rate of TiO_2/Ag/CD in MB degradation can be attributed to the higher concentration of CD and the presence of silver in its structure.

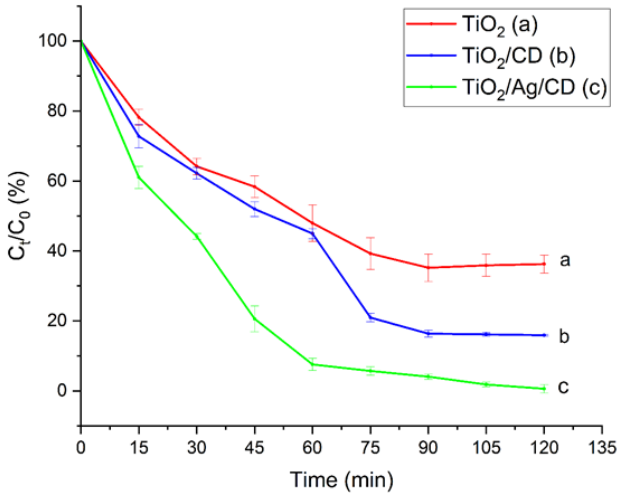

Figure 12: Investigating the effect of photocatalyst, at 0.01 g photocatalyst, 10 ppm MB, 100 mL, 120 min

Table 4: Investigating the effect of photocatalyst

Catalyst	Dosage	Color concentration (ppm)	Time (min)	Degradation (%)
TiO_2	0.01 g/ 100 mL	10	120	63.76
TiO_2/CD	0.01 g/ 100 mL	10	120	84.10
TiO_2/Ag/CD	0.01 g/ 100 mL	10	120	99.38

Investigating the Kinetics of MB Photocatalytic Degradation Reaction

To provide useful information about the effectiveness of the photocatalyst, and subsequently develop the optimal conditions for the ongoing removal of MB by TiO_2/Ag/CD at an industrial level the kinetic models were investigated. Two well-known kinetic models of pseudo-first-order and second-order were applied at variable times from 15 to 120 min and the results are presented in Table 5. The linear plot of kinetic models for the photocatalytic degradation of MB on TiO_2/Ag/CD is indicated in Figure 13, and their derived parameters are illustrated in Table 5. According to the outcomes, the pseudo-second-order model demonstrated excellent linearity with correlation coefficients of 1.00 for photocatalytic removal of MB onto TiO_2/Ag/CD.

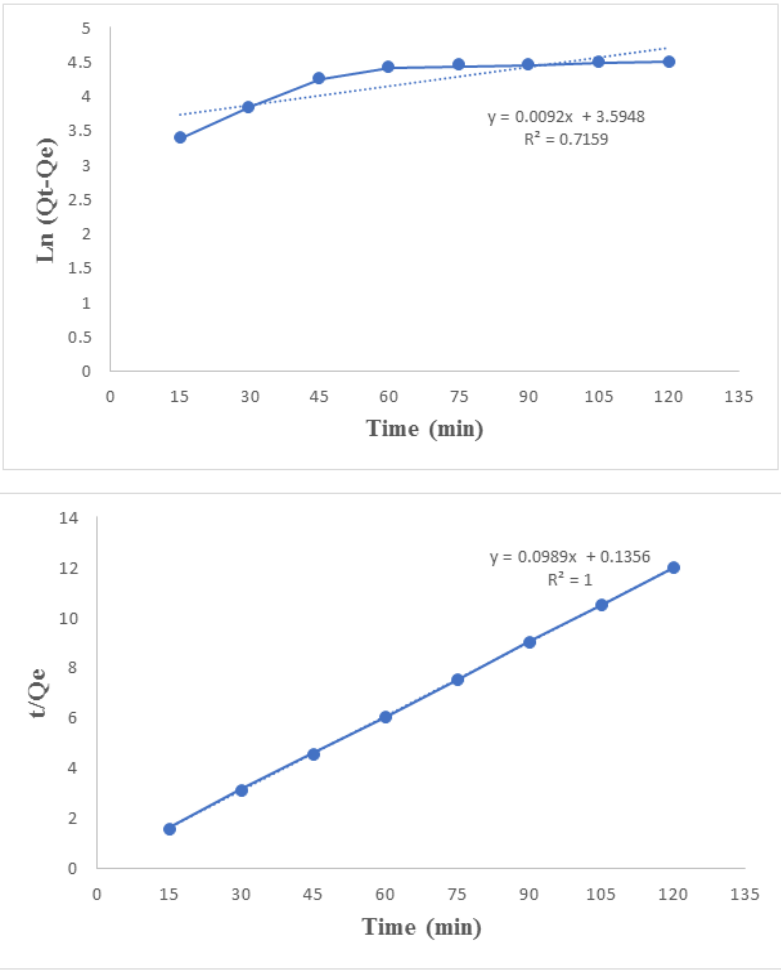

Figure 13: The linear equation of the first degree and the second degree are shown respectively

Table 5: The kinetics parameters for photocatalytic degradation of methylene blue onto TiO_2/Ag/CD composites

Kinetic model	Pseudo-first-order	Pseudo–second–order
R^2	0.7159	1

TiO_2/Ag/CD Recycling

Catalyst recycling is one of the primary concerns for practical applications. The stability of TiO_2/Ag/CD as a photocatalyst for MB degradation was thus investigated. To better investigate the recovery of the photocatalyst, the photocatalytic dye degradation reaction was carried out on a larger scale. For this purpose, one liter of 10 ppm solution of MB was prepared, and then 100 mg of TiO_2/Ag/CD was dispersed in it, and after stirring in the dark for one hour, it

was exposed to sunlight. Experiments on repeatability were conducted for eight continuous cycles. After each run, the catalyst was recovered by washing with water and ethanol and drying at 80 ˚C for one day before the subsequent cycle. After eight cycles, the results indicate that the catalytic efficacy remains essentially unchanged and the MB degradation is maintained at 93.08%. The stability of photocatalyst up to eight consequitive cycles could be because of covalently bounded CD to the modified TiO_2/Ag NPs. During photocatalysis, a few TiO_2/Ag/CD particles are leached into the solution, which contributes to the modest decrease in degradation (Figure 14).

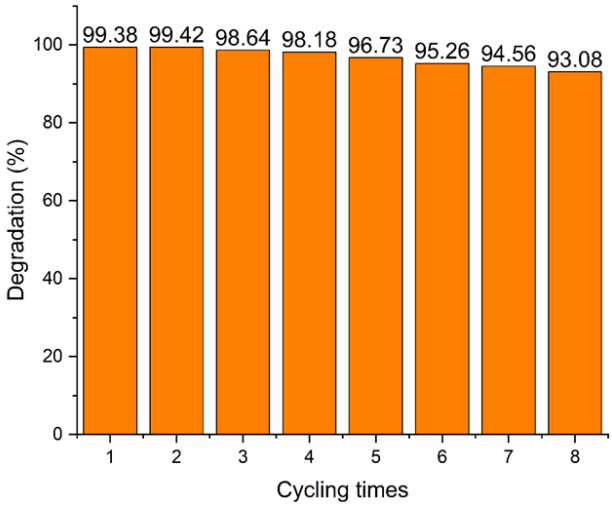

Figure 14: Reusability of the TiO_2/Ag/CD catalyst for the photodegradation of MB, under optimal conditions (100 mL, 10 ppm, 0.01 g TiO_2/Ag/CD, 120 min)

Conclusion

With the aid of a plant extract, TiO_2 and TiO_2/Ag nanoparticles were synthesized, and their surfaces were modified by forming a chemical bond with a silane agent. The modified products were used to create TiO_2/CD and TiO_2/Ag/CD nanocomposites, and then it was demonstrated that the TiO_2/Ag/CD nanocomposite has superior photocatalytic properties compared to the other two photocatalysts under the same conditions, degrading MB dye up to 99.38% under sunlight irradiation. Under the same conditions, synthesized TiO_2 nanoparticles and TiO_2/CD nanocomposite destroyed 63.76 % and 84.1% of the dye, respectively. This is explained because the TiO_2/Ag/CD nanocomposite structure contains silver. It was demonstrated that using DRS analysis that doping silver to TiO_2 nanoparticles causes the reduction of the energy gap from 3.2 eV to 2.5 eV, facilitating simpler electron transfers. This increases the photocatalytic activity of TiO_2. TGA analysis confirmed that the TiO_2/Ag/CD structures contained more CD than the TiO_2/CD nanocomposite. Higher amounts of CD provide a larger substrate (MB dye) adsorption on the photocatalyst surface, thus more MB is available for decomposition by TiO_2, and the presence of silver reduces the amount of energy required by TiO_2 for dye decomposition. The results of this study revealed that the TiO_2/Ag/CD nanocomposite with a lower energy gap and higher content of CD makes it a potential photocatalyst for the degradation of pollutants in aqueous solutions. The order of photocatalytic activity was evaluated to be: TiO_2/Ag/CD > TiO_2/CD > TiO_2-NPs. The results of this research revealed that the synthesized nanocomposite can be used to remove various other organic pollutants. This is under investigation in our laboratory and the results will be reported

shortly. Besides, the antibacterial and anticancer activity of the nanocomposite TiO_2/Ag/CD are under investigation.

Acknowledgments

The authors are thankful to the University of Mazandaran for partial support of this project.

Disclosure Statement

No potential conflict of interest was reported by the authors.

Funding

This study did not receive any specific grant from funding agencies in the public, commercial, or not-for-profit sectors.

Authors' Contributions

All authors contributed toward data analysis, drafting, and revising the article and agreed to be responsible for all aspects of this work.

Conflict of Interest

The authors declare that there is no conflict of interest in this study.

ORCID

Amirhosein Zamani
https://orcid.org/0000-0002-3934-4826
Sakineh Asghari
https://orcid.org/0000-0002-6608-9525
Mahmood Tajbakhsh
https://orcid.org/0000-0002-4856-1937

References

[1]. Zhao Y., Wang G., Li L., Dong X., Zhang X., Enhanced activation of peroxymonosulfate by nitrogen-doped graphene/TiO_2 under photo-assistance for organic pollutants degradation: Insight into N doping mechanism, *Chemosphere*, 2020, **244**:125526 [Crossref], [Google Scholar], [Publisher]

[2]. Moayeripour S.S., Behzadi R., Experimental investigation of the effect of titanium nano-particles on the properties of hydrophobic self-cleaning film. *Journal of Medicinal and Pharmaceutical Chemistry Research,* 2023, **5:**303 [Publisher]

[3]. Sulaiman N.S., Zaini M.A.A., Arsad A., Evaluation of dyes removal by beta-cyclodextrin adsorbent, *Materials Today: Proceedings*, 2021, **39**:907 [Crossref], [Google Scholar], [Publisher]

[4]. Amouzad Mahdiraji E., Kolbadinezhad R., Effects of Establishing Occupational Health and Safety Management Standards and Environmental Management on Environmental Factors and Employee Satisfaction. *Eurasian Journal of Science and Technology,* 2021, **1:**142 [Crossref], [Publisher]

[5]. Basumatary B., Basumatary R., Ramchiary A., Konwar D., Evaluation of Ag@TiO_2/WO_3 heterojunction photocatalyst for enhanced photocatalytic activity towards methylene blue degradation, *Chemosphere*, 2022, **286**:131848 [Crossref], [Google Scholar], [Publisher]

[6]. Kusvuran E., Gulnaz O., Irmak S., Atanur O.M., Yavuz H.I., Erbatur O., Comparison of several advanced oxidation processes for the decolorization of Reactive Red 120 azo dye in aqueous solution, *Journal of Hazardous Materials*, 2004, **109**:85 [Crossref], [Google Scholar], [Publisher]

[7]. Robinson T., McMullan G., Marchant R., Nigam P., Remediation of dyes in textile effluent: a critical review on current treatment technologies with a proposed alternative, *Bioresource Technology*, 2001, **77**:247 [Crossref], [Google Scholar], [Publisher]

[8]. Annadurai G., Chellapandian M., Krishnan M., Adsorption of reactive dye on chitin, *Environmental Monitoring and Assessment*, 1999, **59**:111 [Crossref], [Google Scholar], [Publisher]

[9]. Huang J., Cao Y., Liu Z., Deng Z., Wang W., Application of titanate nanoflowers for dye removal: A comparative study with titanate nanotubes and nanowires, *Chemical Engineering Journal*, 2012, **191**:38 [Crossref], [Google Scholar], [Publisher]

[10]. Sismanoglu T., Kismir Y., Karakus S., Single and binary adsorption of reactive dyes from aqueous solutions onto clinoptilolite, *Journal of Hazardous Materials*, 2010, **184**:164 [Crossref], [Google Scholar], [Publisher]
[11]. Jeni J., Kanmani S., Solar nanophotocatalytic decolorisation of reactive dyes using titanium dioxide, *Journal of Environmental Health Science & Engineering*, 2011, **8**:15 [Google Scholar], [Publisher]
[12]. Sabaghi V., Jalaly M., Rahsepar F., Photocatalytic degradation of industrial pigments by mil-125 derived porous Titanium Dioxide (TiO_2) nanoparticles, *Journal of Medicinal and Nanomaterials Chemistry,* 2020, **2:**300 [Crossref], [Google Scholar], [Publisher]
[13]. Fujishima A., Honda K., Electrochemical photolysis of water at a semiconductor electrode, *Nature*, 1972, **238**:37 [Crossref], [Google Scholar], [Publisher]
[14]. Lin X., Li Y., Preparation of TiO_2/Ag [BMIM] Cl composites and their visible light photocatalytic properties for the degradation of rhodamine B, *Catalysts*, 2021, **11**:661 [Crossref], [Google Scholar], [Publisher]
[15]. Allaedini G., Tasirin S.M., Comparison of TiO_2 nanoparticles impact with TiO_2/CNTs nano hybrid on microbial community of staphylococcus, *Journal of Medicinal and Nanomaterials Chemistry,* 2019, **1:**421-424. [Crossref], [Publisher]
[16]. Nguyen C.H., Fu C.C., Juang R.S., Degradation of methylene blue and methyl orange by palladium-doped TiO_2 photocatalysis for water reuse: Efficiency and degradation pathways, *Journal of Cleaner Production*, 2018, **202**:413 [Crossref], [Google Scholar], [Publisher]
[17]. Tayeb A.M., Hussein D.S., Synthesis of TiO_2 nanoparticles and their photocatalytic activity for methylene blue, *American Journal of Nanomaterials*, 2015, **3**:57 [Crossref], [Google Scholar], [Publisher]
[18]. Choi Y., Umebayashi T., Yoshikawa M., Fabrication and characterization of C-doped anatase TiO_2 photocatalysts, *Journal of Materials Science*, 2004, **39**:1837 [Crossref], [Google Scholar], [Publisher]
[19]. Serpone N., Is the band gap of pristine TiO_2 narrowed by anion-and cation-doping of titanium dioxide in second-generation photocatalysts , *ACS Publications*, 2006 [Crossref], [Google Scholar], [Publisher]
[20]. Luttrell T., Halpegamage S., Tao J., Kramer A., Sutter E., Batzill M., Why is anatase a better photocatalyst than rutile?-Model studies on epitaxial TiO_2 films, *Scientific Reports*, 2014, **4**:4043 [Crossref], [Google Scholar], [Publisher]
[21]. Yang H., Zhang K., Shi R., Li X., Dong X., Yu Y., Sol–gel synthesis of TiO_2 nanoparticles and photocatalytic degradation of methyl orange in aqueous TiO_2 suspensions, *Journal of Alloys and Compounds*, 2006, **413**:302 [Crossref], [Google Scholar], [Publisher]
[22]. Ma H., Zheng W., Yan X., Li S., Zhang K., Liu G., Jiang L., Polydopamine-induced fabrication of Ag-TiO_2 hollow nanospheres and their application in visible-light photocatalysis, *Colloids and Surfaces A: Physicochemical and Engineering Aspects*, 2020, **586**:124283 [Crossref], [Google Scholar], [Publisher]
[23]. Thejeel K.A., Abdul Kareem S.A.A.S., Ascar I.F., Hussein M.A., Synthesis of new polymers linked to heterocyclic using zinc oxide with nanostructures extracted from natural sources, *Egyptian Journal of Chemistry*, 2022, **65**:579 [Crossref], [Google Scholar], [Publisher]
[24]. Alsahib S.A., Thejeel K.A., Synthesis of Zinc Oxide (ZnO) and Study on Mechanical Properties of Polymeric Dental Filling [Google Scholar], [Publisher]
[25]. Mittal A., Mari B., Sharma S., Kumari V., Maken S., Kumari K., Kumar N., Non-metal modified TiO_2: A step towards visible light photocatalysis, *Journal of Materials Science: Materials in Electronics*, 2019, **30**:3186 [Crossref], [Google Scholar], [Publisher]
[26]. Na S., Seo S., Lee H., Recent developments of advanced Ti^{3+}-self-doped TiO_2 for efficient visible-light-driven photocatalysis, *Catalysts*, 2020, **10**:679 [Crossref], [Google Scholar], [Publisher]
[27]. Ingrosso C., Esposito Corcione C., Striani R., Comparelli R., Striccoli M., Agostiano A., Curri M.L., Frigione M., UV-curable nanocomposite

based on methacrylic-siloxane resin and surface-modified TiO_2 nanocrystals, *ACS Applied Materials & Interfaces*, 2015, **7**:15494 [Crossref], [Google Scholar], [Publisher]
[28]. Corcione C.E., Ingrosso C., Petronella F., Comparelli R., Striccoli M., Agostiano A., Frigione M., Curri M.L., A designed UV–vis light curable coating nanocomposite based on colloidal TiO_2 NRs in a hybrid resin for stone protection, *Progress in Organic Coatings*, 2018, **122**:290 [Crossref], [Google Scholar], [Publisher]
[29]. Ramanathan R., Bansal V., Ionic liquid mediated synthesis of nitrogen, carbon and fluorine-codoped rutile TiO_2 nanorods for improved UV and visible light photocatalysis, *RSC Advances*, 2015, **5**:1424 [Crossref], [Google Scholar], [Publisher]
[30]. Lu P., Wu F., Deng N., Enhancement of TiO_2 photocatalytic redox ability by β-cyclodextrin in suspended solutions, *Applied Catalysis B: Environmental*, 2004, **53**:87 [Crossref], [Google Scholar], [Publisher]
[31]. Wang G., Wu F., Zhang X., Luo M., Deng N., Enhanced photodegradation of bisphenol A in the presence of *β*-cyclodextrin under UV light, *Journal of Chemical Technology & Biotechnology: International Research in Process, Environmental & Clean Technology*, 2006, **81**:805 [Crossref], [Google Scholar], [Publisher]
[32]. Govindhan P., Pragathiswaran C., Chinnadurai M., A magnetic Fe_3O_4 decorated TiO_2 nanoparticles application for photocatalytic degradation of methylene blue (MB) under direct sunlight irradiation, *Journal of Materials Science: Materials in Electronics*, 2018, **29**:6458 [Crossref], [Google Scholar], [Publisher]
[33]. Kumar D.A., Palanichamy V., Roopan S.M., One step production of AgCl nanoparticles and its antioxidant and photo catalytic activity, *Materials Letters*, 2015, **144**:62 [Crossref], [Google Scholar], [Publisher]
[34]. Almarbd Z., Mutter Abbass N., Synthesis and characterization of TiO_2, Ag_2O, and graphene oxide nanoparticles with polystyrene as a nonocomposites and some of their applications, *Journal of Medicinal and Pharmaceutical Chemistry Research,* 2022, **4:**1033 [Publisher]
[35]. Ruaa M., Alsahib S., Ascar I., Synthesis, Characterization and cyclazation of pyran using Ag_2O nanoparticle from natural source "GINGER", *Iraqi Journal of Agricultural Sciences*, 2021, **52**:1171 [Crossref], [Google Scholar], [Publisher]
[36]. Mousavi S.H., Mohammadi A., A cyclodextrin/glycine-functionalized TiO_2 nanoadsorbent: Synthesis, characterization and application for the removal of organic pollutants from water and real textile wastewater, *Process Safety and Environmental Protection*, 2018, **114**:1 [Crossref], [Google Scholar], [Publisher]
[37]. [45]. Shen J., Li N., Ye M., Supramolecular photocatalyst of RGO-cyclodextrin- TiO_2, *Journal of Alloys and Compounds*, 2013, **580**:239 [Crossref], [Google Scholar], [Publisher]
[38]. Wang G., Wang X., Yu R., Deng N., Photocatalytic degradation of azo dye acid red 14 based on molecular recognition interaction, *Fresenius Environmental Bulletin*, 2008, **17**:1054 [Google Scholar], [Publisher]
[39]. Sharavath V., Sarkar S., Gandla D., Ghosh S., Low temperature synthesis of TiO2-β-cyclodextrin–graphene nanocomposite for energy storage and photocatalytic applications, *Electrochimica Acta*, 2016, **210**:385 [Crossref], [Google Scholar], [Publisher]
[40]. Sulaiman N.S., Zaini M.A.A., Arsad A., Evaluation of dyes removal by beta-cyclodextrin adsorbent. *Materials Today: Proceedings*, 2021, **39**:907 [Crossref], [Google Scholar], [Publisher]
[41]. Yang J.s., Han S.y., Yang L., Zheng H.c., Synthesis of beta-cyclodextrin-grafted-alginate and its application for removing methylene blue from water solution, *Journal of Chemical Technology & Biotechnology*, 2016, **91**:618 [Crossref], [Google Scholar], [Publisher]
[42]. Rajkumari J., Magdalane C.M., Siddhardha B., Madhavan J., Ramalingam G., Al-Dhabi N.A., Arasu M.V., Ghilan A., Duraipandiayan V., Kaviyarasu K., Synthesis of titanium oxide nanoparticles using Aloe barbadensis mill and evaluation of its antibiofilm potential against Pseudomonas aeruginosa PAO1, *Journal of Photochemistry and Photobiology B: Biology*, 2019, **201**:111667 [Crossref], [Google Scholar], [Publisher]

[43]. Khanna P., Singh N., Charan S., Synthesis of nano-particles of anatase-TiO_2 and preparation of its optically transparent film in PVA, *Materials Letters*, 2007, **61**:4725 [Crossref], [Google Scholar], [Publisher]
[44]. Ebrahimzadeh M.A., Naghizadeh A., Amiri O., Shirzadi-Ahodashti M., Mortazavi-Derazkola S., Green and facile synthesis of Ag nanoparticles using Crataegus pentagyna fruit extract (CP-AgNPs) for organic pollution dyes degradation and antibacterial application, *Bioorganic Chemistry*, 2020, **94**:103425 [Crossref], [Google Scholar], [Publisher]
[45]. Jiang L., Zhou G., Facile synthesis of monodispersed nanocrystalline anatase TiO_2 particles with large surface area and enhanced photocatalytic activity for degradation of organic contaminant in wastewaters, *Materials Science in Semiconductor Processing*, 2012, **15**:108 [Crossref], [Google Scholar], [Publisher]
[46]. Zhao J., Milanova M., Warmoeskerken M.M., Dutschk V., Surface modification of TiO_2 nanoparticles with silane coupling agents, *Colloids and Surfaces A: Physicochemical and Engineering Aspects*, 2012, **413**:273 [Crossref], [Google Scholar], [Publisher]
[47]. Fallah Z., Isfahani H.N., Tajbakhsh M., Cyclodextrin-triazole-titanium based nanocomposite: Preparation, characterization and adsorption behavior investigation, *Process Safety and Environmental Protection*, 2019, **124**:251 [Crossref], [Google Scholar], [Publisher]
[48]. Zhang G., Wang J., Zhang H., Zhang, T., Jiang S., Li B., Zhang H., Cao J., Facile synthesize hierarchical tubular micro-nano structured AgCl/Ag/TiO_2 hybrid with favorable visible light photocatalytic performance, *Journal of Alloys and Compounds*, 2021, **855**:157512 [Crossref], [Google Scholar], [Publisher]
[49]. Ma Y.X., Shao W.J., Sun W., Kou Y.L., Li X., Yang H.P., One-step fabrication of β-cyclodextrin modified magnetic graphene oxide nanohybrids for adsorption of Pb (II), Cu (II) and methylene blue in aqueous solutions, *Applied Surface Science*, 2018, **459**:544 [Crossref], [Google Scholar], [Publisher]
[50]. Bezrodna T., Puchkovska G., Shymanovska V., Baran J., Ratajczak H., IR-analysis of H-bonded H_2O on the pure TiO_2 surface, *Journal of Molecular Structure*, 2004, **700**:175 [Crossref], [Google Scholar], [Publisher]
[51]. Gogoi D., Namdeo A., Golder A.K., Peela N.R., Ag-doped TiO_2 photocatalysts with effective charge transfer for highly efficient hydrogen production through water splitting, *International Journal of Hydrogen Energy*, 2020, **45**:2729 [Crossref], [Google Scholar], [Publisher]
[52]. Fallah Z., Isfahani H.N., Tajbakhsh M., Mohseni M., Zabihi E., Abedian Z., Antibacterial and cytotoxic effects of cyclodextrin-triazole-titanium based nanocomposite, *Brazilian Archives of Biology and Technology*, 2021, **64**:e21190750 [Crossref], [Google Scholar], [Publisher]
[53]. Attarchi N., Montazer M., Toliyat T., Ag/TiO_2/β-CD nano composite: preparation and photo catalytic properties for methylene blue degradation, *Applied Catalysis A: General*, 2013, **467**:107 [Crossref], [Google Scholar], [Publisher]
[54]. Jiang L., Zhou G., Mi J., Wu Z., Fabrication of visible-light-driven one-dimensional anatase TiO_2/Ag heterojunction plasmonic photocatalyst, *Catalysis Communications*, 2012, **24**:48 [Crossref], [Google Scholar], [Publisher]
[55]. Jiang C., Liu W., Yang M., Zhang F., Shi H., Xie Y., Wang Z., Robust fabrication of superhydrophobic and photocatalytic self-cleaning cotton textiles for oil–water separation via thiol-ene click reaction, *Journal of Materials Science*, 2019, **54**:7369 [Crossref], [Google Scholar], [Publisher]
[56]. Meng Y., A sustainable approach to fabricating Ag nanoparticles/PVA hybrid nanofiber and its catalytic activity, *Nanomaterials*, 2015, **5**:1124 [Crossref], [Google Scholar], [Publisher]
[57]. Uboncholakate K., Sikong L., Saito F., Photocatalytic disinfection of P. aeruginosa bacterial Ag-doped TiO_2 film, *Procedia Engineering*, 2012, **32**:656 [Crossref], [Google Scholar], [Publisher]
[58]. Shirke B., Korake P., Hankare P., Bamane S., Garadkar K., Synthesis and characterization of pure anatase TiO_2 nanoparticles, *Journal of*

Materials Science: Materials in Electronics, 2011, **22**:821 [Crossref], [Google Scholar], [Publisher]
[59]. Goncalves M.S., Oliveira-Campos A.M., Pinto E.M., Plasencia P.M., Queiroz M.J.R., Photochemical treatment of solutions of azo dyes containing TiO_2, *Chemosphere*, 1999, **39**:781 [Crossref], [Google Scholar], [Publisher]

Use your device to scan and read the article online

HOW TO CITE THIS ARTICLE
Amirhosein Zamani, Sakineh Asghari, Mahmood Tajbakhsh. Synthesis of TiO_2/CD and TiO_2/Ag/CD Nanocomposites and Investigation of Their Visible Light Photocatalytic Activities in the Degradation of Methylene Blue. *Chem. Methodol.*, 2024, 8(3) 177-199
DOI: https://doi.org/10.48309/CHEMM.2024.432168.1753
URL: https://www.chemmethod.com/article_190858.html